**Proceedings of the 28th IEEE**
**EMBS Annual International Conference**
**New York City, USA, Aug 30-Sept 3, 2006**



# Mechanical Mechanisms for Thrombosis in Microvessels

Qin Liu, David Mirc, and Bingmei M. Fu

*Abstract*— **The hypothesis that thrombus can be induced in curved vessels due to mechanical stimuli was tested both experimentally and computationally. Our *in vivo* experiments on the mesentery of Sprague-Dawley rats (250-300g) showed that thrombi were formed in non-injured curved microvessels (post-capillary venules, 20-50 micrometer in diameter), and they were initiated at the inner side of the vessel. We observed thrombus formation in 7 out of 32 microvessels after they were stretched and curved for 10-60 min. To investigate the mechanical mechanisms of thrombus induction, we performed 3-D computational simulation using commercial software, FLUENT. The blood flow was approximated as a Newtonian laminar flow with Reynolds number around 0.01 in this type of microvessels. We considered the vessels with different curvatures ($90^o$ and $180^o$) as well as different shaped-cross sections (circular and elliptic). Computational results demonstrated that the shear rate and shear rate gradient and at the inner side of the vessel were higher than those at the opposite side. The differences became larger in more bended and elliptic-shaped microvessels. This suggested that higher shear rate and shear rate gradient are two of the factors that initiate the thrombosis in curved post-capillary venules. Our results are consistent with others in branched venules.**

## I. Introduction

Thrombosis is the formation of blood clots within blood vessels. It is a direct cause for a stroke, a myocardial infarction and atherosclerosis. Although both biochemical (e.g. cell adhesion molecules) and mechanical (e.g. stresses and shear rates) factors are found to play a role in thrombosis, the quantitative understanding of their contribution is poor, especially in the non-injured microvasculature with laminar flows. The objective of this study is to investigate the relationships between localized shear rates and stresses in bended/stretched microvessels, and thrombosis in intact microvessels.

It has been found that mechanical factors alone, without exogenous chemical factors, can induce platelet aggregation near an injured/damaged location in the vessel. These mechanical factors are shear stresses/rates, the local geometry of the vessel, and the duration of the applied forces [1], [3], [9], [11], [12]. Increasing the shear rate will increase the attachment of platelets to the vessels wall and the rate of platelet aggregation [19].

Study [18] on rat mesenteric microvessels (arterioles/venules), which were pretreated using irradiation method, showed that thrombus initiation depended significantly on shear rate rather than the flow velocity. Platelet thrombi were initiated at the locations of higher shear rates in venules, and of lower shear rates in arterioles. The relation between thrombus initiation time and shear rate was almost linear. They also observed the same results in arteriolar bifurcations, venular confluences and curved arteriolar/venular vessels of rat mesentery. Study on T-type arteriolar bifurcations [11] showed significant shear rate gradients occurred at the branch locations in both the axial and radial directions.

While previous studies have led to a better understanding of the mechanical mechanism of thrombus formation, all these studies have been conducted under the conditions that either the flow is retarded (flow stasis) or the flow is disturbed (secondary flow), or the vessels are injured/damaged by using mechanical, electrical, chemical, laser-induced [17] or photochemical means [16]. In our proposed project, we want to test the hypothesis that thrombi can be formed in a laminar blood flow with normal circulation and in normal microvessels, which are bent/stretched but non-injured, solely by the mechanical stimuli, such as localized stresses and shear rates.

## II. Material and Methods

### A. Experimental Method

Experiments were performed on rat mesenteries. All procedures and animals use have been approved by the Animal Care and Use Committees at University of Nevada-Las Vegas. Female Sprague-Dawley rats (250-300 g) were supplied by Simonson Laboratory (Gilroy, CA). Rats (age 3-4 months) were anaesthetized with pentobarbital sodium given subcutaneously. After a rat was anesthetized, a midline surgical incision (2-3 cm) was made in the abdominal wall. The rat was then transferred to a tray and kept warm on a heating pad [4]. The mesentery was gently taken out from the abdominal cavity and arranged on the surface of a polished quartz pillar (2cm in diameter, Heræus-Amersil, Fairfield, NJ) to maintain the circulation to the gut and mesentery of the animal. The upper surface of the mesentery was continuously superfused by a dripper with Ringer solution at 35-37 $^oC$, which was regulated by a controlled water bath and monitored regularly by a

Manuscript submitted April 24, 2006. This work was supported by National Science Foundation CAREER and REU grants, and Science Fellowship of the City University of New York.

Q. Liu is with the Department of Biomedical engineering, The City College of The City University of New York, NY 10031 USA (email: liuqin@engr.ccny.cuny.edu).

D. Mirc, was with the Department of Mechanical Engineering, University of Nevada, Las Vegas, NV 89154 USA.

B.M. Fu was with University of Nevada, Las Vegas, NV 89154 USA. She is now with the Department of Biomedical engineering, The City College of The City University of New York, NY 10031 USA (phone: 212-650-7531; fax: 212-650-6727; email: fu@ccny.cuny.edu).

thermometer probe. The flow of superfusate was maintained at 3.5-4.0 ml/min and this kept the layer of fluid over the tissue at approximately constant depth. A Nikon Eclipse TE-300 inverted microscope with a 10× lens (NA 0.3, Nikon) or 20× (NA 0.35, Nikon) was used to observe the mesentery. The microvessels chosen for study were straight non-branched post-capillary venules (diameters 20-50 μm). All vessels had brisk blood flow and had no marginating white cells before they were bended and stretched.

With the mesentery and a chosen microvessel under observation, a rounded-tip glass restraining micropipette (see arrow in Fig.1) was used to bend and stretch the microvessel at the nearby tissue. Cautions were taken during the manipulation to induce no/minimum damages to the vessels. Blood circulation in the microvessel was observed by using a COHU CCD video camera.

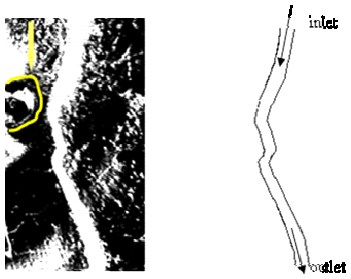


(a) (b)

Fig. 1 (a) A single mesenteric microvessel curved by a restraining micropiptte. The location of the restraining pipette is shown by the arrow. (b) The sketch for the curved vessel and the blood flow directions.

*B. Numerical Method*

The 3-D microvessel geometry was created by using SolidWorks (SolidWorks Corp., Concord, MA). The curvature in the microvessel model was about 90°, similar as that observed in the experiment. Two different curvature angles, 0° (straight) and 180°, and elliptic cross section were created for comparison. The total length of the microvessel was 350 μm. The diameter of circular cross section of was 25 μm. By assuming microvessel wall to be rigid, cross section perimeter $c$ was unchanged. A characteristic elliptic cross section with the long radius $a$ twice of the short radius $b$ ($a = 2b$) was chosen. Using Eq. 1, we had $a$ = 16.2 μm and $b$ = 8.1 μm. The geometry of vessel models was shown in Fig. 2.

$$c = \pi \cdot [\frac{3}{2} \cdot (a+b) - \sqrt{ab}] \quad (1)$$

Microvessel model geometries were then exported to Gambit, a CFD preprocessor (Fluent Inc., Lebanon, NH), for meshing. Approximately 600k – 700k hexahedral elements were generated for the curved vessel with circular cross section and 1.5 million elements were generated for vessel with elliptic cross. Meshed models were then exported to Fluent (Fluent 6.1.22, Fluent Inc., Lebanon, NH). Conservation of mass equation and momentum equation (Navier-Stokes) were solved by using Fluent. Blood flow in the vessel was assumed to be steady, incompressible, laminar, and Newtonian with average velocity 1 mm /s (measured velocity in this type of microvessels). Microvessel wall was assumed to be rigid and impermeable. The density of blood was 1050 kg/m$^3$, and viscosity 2.5 cP [7]. Non-slip boundary condition was applied on the wall. The outlet pressure was 980 Pa (10cm $H_2O$, average measured value) and inlet pressure was determined by using trial-and-error method so that the average velocity in the vessel was 1 mm/s. The Reynolds number of the flow in the vessel was approximately 0.01. Solution convergence criterion was $10^{-8}$ in magnitude of residuals. Computations were performed on a personal computer (DELL, Pentium 4 CPU, 3.80GHz, 3.37GB RAM) and each case typically lasted about 8 hours.

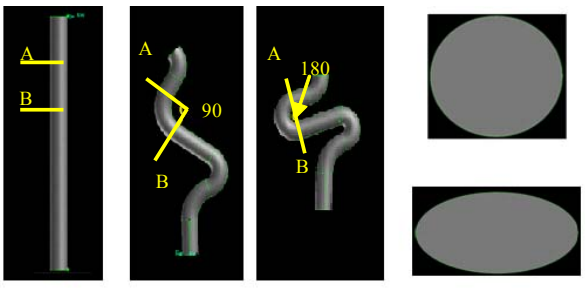


(a) (b)

Fig. 2 Illustration of various model geometries. (a) shows 3 different curvatures. Cross section A is at upstream and B downstream. The distances from inlet to cross section A for all these cases are the same. The midline lengths of section AB in these models are also the same. (b) shows 2 different cross sections. Circular cross section is shown on the top, the radius is 12.5 μm. Elliptic cross section is shown at the bottom, in which the long radius is 16.2 μm and the short radius 8.1 μm.

## III. Results

*A. Experimental Result*

We tested 32 post-capillary venules in rat mesenteries. We observed that thrombi were initiated at the inner side of the curved vessels in 7 of 32 vessels (indicated by the

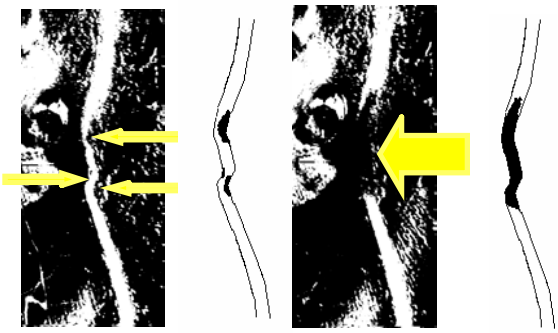

(a) (b)

Fig. 3 (a) After the vessel was stretched and curved for ~10 minutes, blood cells began to accumulate at the inner side of the curvature. Arrows show the initiation locations of thrombi. (b) several minutes later, the vessel was completely blocked. Figures on the left are photos taken in the experiment, on the right are sketches of the experimental observations

arrows in Fig. 3a) after the vessels were bended/stretched for ~10-60 minutes. 3 vessels were completely blocked in as soon as 7 minutes (big arrow in Fig. 3b). 4 vessels had visible thrombi that did not occlude the circulation. Although there were no (or minimum) injuries to the vessels in our in vivo experiments, the thrombi still formed in 22% of the vessels and the complete occlusion happened in 9.4% of the vessels.

*B. Computational Results*

In Fig. 4, we plot the velocity profiles as a function of angular coordinate θ along the longitudinal axis. The origin of the coordinate is located at the apex of the bended portion of the vessel (Fig. 2). Figures 4a, b, and c are for the vessels with the circular cross section when the bended angles are $0^o$ (straight), $90^o$ and $180^o$. Figures 4d, e, and f are for the corresponding vessels with the elliptic

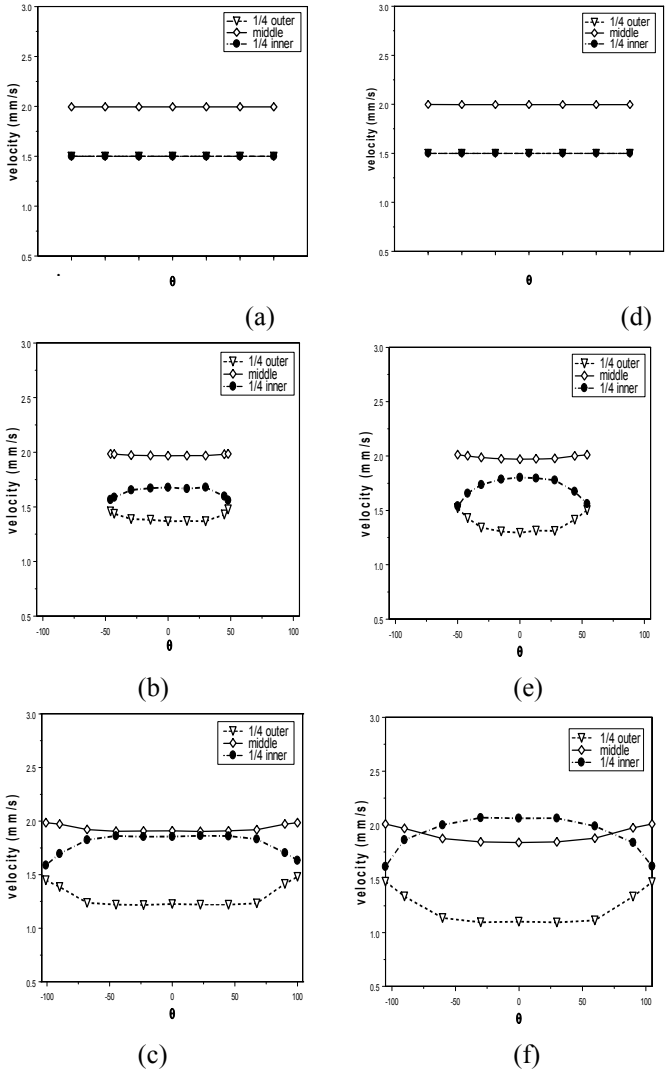


Fig. 4 Velocity profiles at the curved portions. (a)-(c) are vessels with circular cross section, (d) – (e) are vessels with elliptic cross section.

cross section. Velocities are plotted for the middle-line (the solid line with the diamonds), the line ¼ vessel diameter far

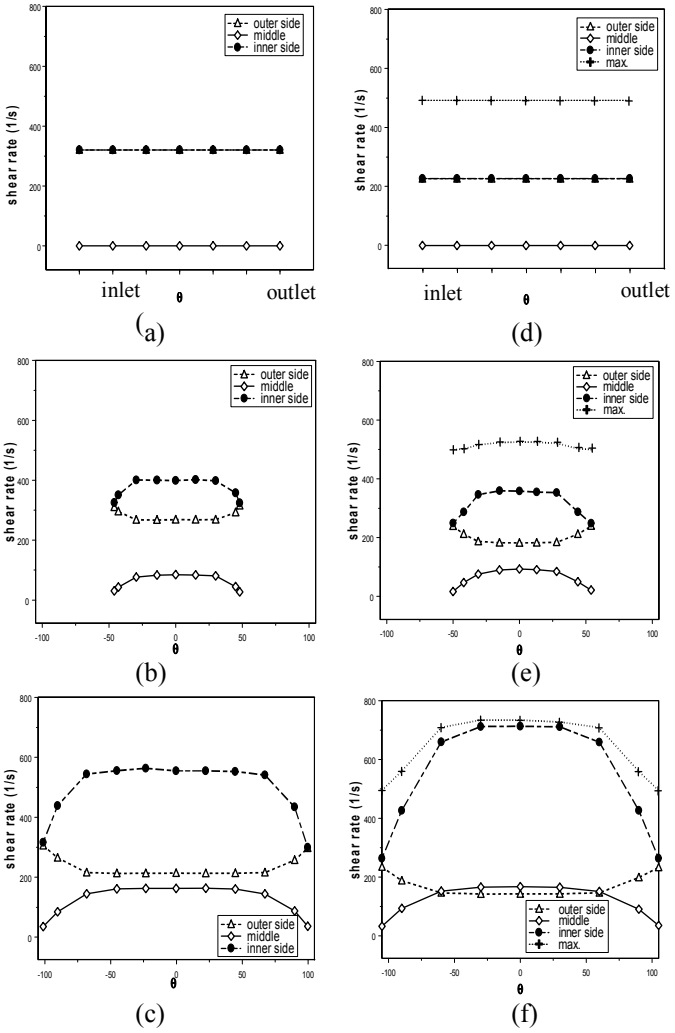


Fig. 5 Shear rate profile at curved locations. (a) – (c) are vessels with circular cross section, (d) – (e) are vessels with elliptic cross section.

from the inner (the dash-dot-dash line with the circles) and the line ¼ vessel diameter far from the outer (the dashed line with the triangles) walls. For the straight vessels, the maximum velocity is constant along the centerline and the velocities at ¼ diameter inner and outer lines are overlapped. For the bended vessels, the centerline velocity is no longer constant. It decreases from the straight portion towards the bended portion, with the minimum at the most bended point. The larger the bending angle, the smaller the velocity at the most bended point. However, the velocity along the ¼ diameter inner line increases from the straight part to the bended part, with the most increase in the transition region from the straight to the curved portions. Along about half of the curved portion, the velocity is almost constant. This constant is smaller than that along the centerline for the less bended vessels, but becomes closer to the centerline value as the bending angle becomes larger or the cross section becomes elliptic. It almost overlaps with the centerline velocity for the $180^o$ bended vessel with the circular cross section (Fig. 4c) and overpasses the centerline velocity for the elliptic shaped vessel (Fig. 4f). In contrast, the velocity at the ¼ diameter outer line decreases from the straight to the bended portions. The decreasing rate is almost

the same as the increasing rate for the velocity along the ¼ diameter inner line at the transition region. The velocity at the ¼ diameter outer line is also constant along about half of the curved portion. The difference between the two constant velocities for the inner and outer lines becomes bigger when the bending angle becomes larger, or the cross section deviates more from the circular shape.

Figure 5 shows the shear rate profiles as a function of θ along the centerline (the solid line with the diamonds) and the inner (the dash-dot-dash line with circles) and outer (the dashed line with triangles) walls. The maximum shear rate at each cross section (the dotted line with crosses) for the elliptic shaped vessel is also plotted as a function of θ. In the straight vessels, the minimum shear rate (or shear) at each cross section occurs at the centerline while the maximum occurs at the walls. For the elliptic shaped vessel, the maximum shear rate is at the apex of the shorter axis. The values of these shear rates are constant along the centerline and along the walls. However, when the vessels are bended, the shear rates at the centerline, at the inner wall, as well as the maximum shear rate for the elliptic shaped vessel, increase from the straight to the bended portions during the transition, reach a plateau for about half part of the curved segment, and then decrease at the same rate as for the increase. However, the shear rate at the outer wall behaves in an opposite way. The larger the bending angle, the higher the increase/decrease rate, the larger the plateau rate at the inner wall, the larger the difference between the plateau rates at the inner and the outer walls, and the larger the maximum shear rate for the curved elliptic shaped vessels. The maximum shear rate for the elliptic shaped vessels occurs at two locations symmetric to the innermost point of the wall.

## IV. Discussion

To investigate the mechanical mechanisms by which thrombi are initiated in the curved microvessels with normal blood circulation, we used 3-D numerical simulation to calculate the detailed distribution of velocity, pressure (not shown), and shear rate in the microvessels with different curvatures and cross-sectional shapes. In our simulation, we have assumed that 1) the flow is laminar, 2) the blood is incompressible, 3) the blood is Newtonian fluid with the constant viscosity, 4) the vessel wall is rigid, and 5) the wall is impermeable. In post-capillary venules, Reynolds number is in the order of 0.01, the first two assumptions are satisfied. Previous studies in [6], [13] indicated that the influence of shear rate on viscosity appears to be small for the shear rates in the microcirculation under normal conditions. Therefore the third assumption is valid. The fourth assumption is reasonable in our study for normal blood pressure. We also confirmed this by observing no changes in the vessel diameter during the experiment. Compared to the flow inside the vessel, the flow across the vessel wall is negligible ($10^{-5}$ of the flow in the vessel) under normal conditions. When the vessel is damaged due to a variety of stimuli under pathological conditions, the flow across the wall can be increased dramatically and we will consider a permeable wall in the future study.

In summary, our combined in vivo experimental study (Fig. 3) and numerical simulation (Figs.4, 5) indicated that the localized velocities, shear rates and shear rate gradients can induce thrombi in microvessels under normal physiological conditions. The possible explanation is that the increased shear rates/gradients activate the endothelial cells forming the microvessel wall and activate the platelets in the blood to increase the adhesion and accumulation of the platelets.

## References


[1] G. Abelsethe, R.E. Buckley, G.E. Pineo, R. Hull and M. Rose, Incidence of deep vein thrombosis in patients with fractures of the lower extremity distal to the hip. J. Orthopedic Trauma. 10(1996), 230-235.

[2] L. Goubergrits, K. Affeld, E. Wellnhofer, R. Zurbrugg and T. Holmer, Estimation of wall shear stress in bypass grafts with computational fluid dynamics method. Int J Artif Organs. 24(2001), 145-151.

[3] E.F. Grabowski, Thrombolysis, flow and vessel wall interactions, J. Vasc. Interv. Radiol., 6 (1995), 25S-29S.

[4] P. He, M. Zeng and F.E. Curry, cGMP modulates basal and activated microvessel permeability independent of [Ca2+]i. Am. J. Physiol.: Hear Circ. Physiol. 274(1998): H1865-H1874.

[5] P.A. Holme, U. Ørvim et. al. Shear-induced platelet activation and platelet microparticle formation at blood flow conditions as in arteries with a severe stenosis. Arterioscler. Thromb. Vasc. Biol., 17(1997), 646-653.

[6] B.E. Iordache and A. Remuzzi, Numerical analysis of blood flow in reconstructed glomerular capillary segments. Microvascular Res. 49(1995), 1-11.

[7] J. Levenson, P. Flaud, M.D. Pino and A. Simon, Blood viscosity as a chronic contributing factor of vasodilatation in humans. J. Hypertension. 8(1990), 1049-1055.

[8] Y. Liu, K. Pekkan, S.C. Jones and A.P. Yoganathan, The effects of different mesh generation methods on computational fluid dynamic analysis and power loss assessment in total cavopulmonary connection. J Biomech. Eng. 126(2004), 594-603.

[9] K.M. Muga, L.G. Melton and D.A. Gabriel, A flow dynamic technique used to assess global hemostasis. Blood Coag Fibrin. 6(1995), 73-78.

[10] S. Murata, Y. Miyake and T. Inaba, Laminar flow in a curved pipe with varying curvature. J. Fluid Mech. 73(1976), 735-752.

[11] D. Noren, H.J. Palmer and M.D. Frame, Predicted wall shear rate gradients in T-type arteriolar bifurcations. Biorheology. 37(2000), 325–340.

[12] O'Brien Jr., Shear-induced platelet aggregation. Lancet. 335(1990), 711-713.

[13] A.R. Pries, D. Neuhaus and P. Gaehtgens, Blood viscosity in tube flow: dependence on diameter and hematocrit. Am J Physiol. 263(1992), H1770-1778.

[14] W.H. Reinhart, Shear-dependence of endothelial functions. Experientia. 50(1994), 87-93.

[15] A.J. Roberts, Shear dispersion along circular pipes is affected by bends, but the torsion of the pipe is negligible. SIAM J. Applied Dynamical Systems. 3(2004), 433-462.

[16] M. Rucker, et. al., New model for in vivo quantification of microvascular embolization, thrombus formation and recanalization in composite flaps. J. Surg. Res. 108(2002), 129-137.

[17] T. Sasaki, M. Kuzuya, X.W. Cheng and K. Nakamura, A novel model of occlusive thrombus formation in mice. Lab Invest. 84(2004), 1526-1532.

[18] M. Sato and O. Norio, Effect of wall shear rate on thrombogenesis in microvessels of the rat mesentery. Circulation Research. 66(1990), 941-949.

[19] V. Turitto and C. Hall, Mechanical factors affecting hemostasis and thrombosis. Thrombosis Research. 92(1998), S25-31.